Medium Effects on the Reductive Cleavage of the Carbon−Halogen Bond in Methyl and Methylene Halides

ARTICLE *in* THE JOURNAL OF PHYSICAL CHEMISTRY B · FEBRUARY 2001

Impact Factor: 3.3 · DOI: 10.1021/jp003646m

3 AUTHORS, INCLUDING:

Milan Fedurco
Michelin Switzerland
54 PUBLICATIONS **2,843** CITATIONS
SEE PROFILE

Jan Augustynski
University of Geneva
111 PUBLICATIONS **3,893** CITATIONS
SEE PROFILE

Ab Initio and Electrochemical Studies on the Reductive Bond Dissociation in Haloethanols

Milan Fedurco,* Laurence Coppex, and Jan Augustynski

Department of Chemistry, University of Geneva, CH 1211 Geneva 4, Switzerland

Received: August 25, 2001; In Final Form: December 17, 2001

Electrochemical behavior of two water-soluble molecules, namely, 2-bromoethanol (Br-EtOH) and 2-iodoethanol (I-EtOH), on glassy carbon and on group IB metal electrodes is investigated. Because the carbon−halogen (C−X) bond cleavage in these haloethanols is a totally irreversible process, the corresponding redox potentials were determined from the ab initio calculations and/or from the known C−X bond dissociation energy in these molecules. The gas phase Gibbs energies of formation for the reactants and the reaction products were obtained at the MP2/6-31G** level and were further corrected for the hydration of molecules using the Polarization continuum model (PCM) extended for the calculations of polarization, repulsion and cavitation contributions to the total solvation energy. The overvoltage for the I-EtOH reduction on Ag(111) and polycrystalline Ag is shown to be approximately 0.4 V lower than on glassy carbon electrode. The electroreduction of I-EtOH at Cu(111) and Cu(100) electrodes takes place at potentials only slightly more negative than that on silver. In all cases, the observed overvoltages are much lower than those predicted by the current dissociative electron transfer model. Gas chromatographic analyses revealed ethylene being the major reaction product, with only small amounts (4−10%) of ethanol formed during the bulk electrolysis runs resulting practically in a complete destruction of iodoethanol.

I. Introduction

Carbene and methyl radical are the likely intermediates in various electrochemical reactions such as, for example, reduction of carbon dioxide[1] and cyanides[2] on copper. Recently, we have described a method allowing to generate large amounts of CH_2 and $\cdot CH_3$ radicals at the electrode/aqueous solution interface virtually in the absence of H_2 evolution.[3] Accordingly, we have been able to study in neutral solutions the reactivity of the CH_2 and $\cdot CH_3$ species on silver and copper, in comparison with that at a glassy carbon electrode. As a suitable source of these radicals we used CH_3X and CH_2X_2 (where X= I, or Br) compounds, having largely differing energy requirements for the dissociative C−X bond cleavage. We found that the methyl and methylene iodides possesing low-lying LUMO orbital, and relatively low dissociation energies ($D_o \approx 240$ kJ/mol), undergo reduction in an aqueous solvent to C_1-C_2 hydrocarbons much easier than their brominated analogues ($D_o \approx 280-320$ kJ/mol).[4] Because of the involvement of the metal surface in the electrode process (inner-shell electron transfer), the reduction of CH_2I_2, CH_2Br_2 and CH_3I on polycrystalline Ag or Cu electrodes takes place over a relatively large potential range from −0.5 to −1 V vs NHE. Under such conditions, the electrogenerated carbene and methyl radicals get stabilized by adsorption on the positively charged metal surface. One of the main conclusions reached in ref 3 is that the positively charged electrode surface favors radical recombination pathways (to form ethylene, or ethane), whereas methane formation (carbanion chemistry) predominates at the negatively charged metal (and carbon) electrodes. Interestingly, the electroreduction of halocarbons in 1 M aq. $NaClO_4$ solutions to form methane, takes place at potentials ca. 2 V more positive than in *N*,*N*-dimethylformamide (DMF)/0.1 M $TBAPF_6$.[4] This suggests that the related heterogeneous electron-transfer kinetics in water might be many orders of magnitude faster than expected on the basis of the current model of dissociative electron transfer (DET).[5] In the present study, the range of the investigated compounds is extended to highly water-soluble haloethanol molecules, namely, 2-bromoethanol and 2-iodoethanol.

Reduction of Br-EtOH and I-EtOH has previously been studied in DMF solutions on several metal electrodes including polycrystalline Pb and Cu.[6] Practically quantitative Br-EtOH conversion to ethylene and hydrogen (11:1) on a Cu electrode, at ca. −1.9 V vs.SCE, in DMF/TBABr solutions (cation-exchange membrane between the two compartments of the cell, ca. 1−5% H_2O) has been reported. Under slightly different conditions, a radical-coupling chemistry, leading to the formation of $Br(CH_2)_2-O-(CH_2)_2OH$, and other ethers, has been observed in DMF containing less than 1% of water (anion-exchange membrane separating the anodic and cathodic compartments). In addition, ethylene was formed with efficiency of ca. 40%. On the other hand, synthesis of 1,4-butanediol has been observed following the cleavage of 2-iodoethanol and 2-bromoethanol on glassy carbon in DMF or acetonitrile catalyzed by Ni(II)- or CoII)-salene complexes (up to 40% yield).[7] The recombination of hydroxyethyl radicals ($\cdot CH_2CH_2OH$) to form 1,4-butanediol has also been reported to occur in NH_4OH solutions at a Cu cathode (Nafion-divided cell), in the presence of Cu(II) ions in the catholyte.[8]

On the other hand, thermally induced decomposition of 2-iodoethanol on a Ag(110) surface in gas phase (263−340 K) has been reported[9] to result in hydroxyethyl intermediate, which further undergoes β-hydride elimination and C−O scission to yield acetaldehyde, ethylene, water, and ethanol. Ethylene and acetaldehyde have also been recently identified as main reaction

* To whom correspondence should be addressed.

10.1021/jp013299w CCC: $22.00
Published on Web 02/09/2002

products during the thermally induced 2-bromoethanol cleavage on Ag(111) in the gase phase.[10]

This type of "destructive" surface chemistry of $\cdot CH_2CH_2OH$ radical is contrasted by a practically quantitative recombination of methyl radicals (thermally or photochemically generated from methyl halides) on group IB metals to produce ethane, or that of ethyl radicals to give butane.[11,12] In fact, the 1,4-butanediol formation has never been noticed in the gas-phase studies dealing with thermal activation of haloethanols on metal surfaces.

In the present work, 2-bromoethanol and 2-iodoethanol were used to test the effect of metal and, specifically, its crystallographic orientation on the rate of dissociative bond cleavage, assisted by the metal surface (inner-shell ET). This study was prompted by the results of gas-phase experiments reported by Bent,[11,12] showing approximately 100 times faster recombination rates of adsorbed $\cdot CH_3$ radicals to form ethane on Cu(100) as compared to Cu(110).

II. Experimental Part

All solutions were freshly made from analytical reagent grade chemicals and high purity water (18.2 MΩ resistivity, Millipore). 2-bromoethanol (Br-EtOH), 2-iodoethanol (I-EtOH) and CH_3I were obtained from Fluka. Measurements were performed in a two-compartment glass cell. A platinum counter-electrode (large area Pt grid) was separated from a working electrode by a ceramic frit. A cross section of low-index single crystals rods (3 mm in diameter): Cu(111), Cu(100), Cu(110), and Ag(111) (oriented with 0.5° accuracy, Metal Crystals & Oxides, Ltd), or polycrystalline Ag and Cu rods, 3 mm in diameter (Specpure 99.999%, Johnson Matthey), served as working electrodes. Small glassy carbon electrode, $d = 3$ mm (Metrohm) and, in the case of bulk electrolyses of haloethanols, a larger glassy carbon rod, $d = 7$ mm (Sigradur K, both embedded in Teflon), were also used as working electrodes. The electrode surface was prepared by polishing mechanically with fine emery papers and then with suspensions of 1.0 μm and 0.3 μm alumina powders. Alumina was removed from the electrode surface via gentle sonication in an ultrasonic bath and washing with copious amount of distilled water. Before the measurements, the electrode surface was cleaned by cycling the potential into the hydrogen evolution region (two voltammetric scans from −0.4 V to −1.8 V and back in 1 M $NaClO_4$ solution). All potentials were measured against a Ag/AgCl/Cl^- reference electrode and are reported versus NHE. Electrochemical measurements were performed in deaerated solutions, under argon atmosphere, at 22 ±1 °C.

All electrochemical experiments on copper were conducted in 0.01 M phosphate buffer/0.1 M $NaClO_4$ solutions (pH 6.45) because, even in neutral unbuffered solutions, copper single-crystal electrodes can easily get covered by a thin layer of a surface oxide.[13] Finally, phosphate was preferred over acetate buffer because of serious decomposition of the latter in the anodic compartement of the electrochemical cell (on a Pt anode), which interfered with analyses of gaseous reaction products coming from the haloethanol reduction. The latter were performed with a Hewlett-Packard 5890 Series II gas chromatograph equipped with a FID and a TCD detectors (Haysep R, respectively, Carbosieves S II columns).

III. Results and Discussion

Figure 1A shows recorded (circles) and simulated (solid line) cyclic voltammograms (CV) for the electroreduction of 5.45 mM I-EtOH and Br-EtOH solutions in 0.125 M $NaClO_4$/0.01 M phosphate buffer (pH 6.45) on a glassy carbon electrode. The CV simulations are discussed in detail in section IIIB. Similar voltammetric behavior was also observed in 0.8 M $NaClO_4$/0.2 M acetate buffer/ (pHs 5, 6, and 7) supporting electrolytes. The electrochemical experiments on haloethanol reduction were restricted to pHs higher than 5 due to the interference from the proton reduction, already perceptible in Figure 1A. Figure 1B shows cyclic voltammogram for 25 mM Br-EtOH in a 0.1 M $NaClO_4$ solution the pH of which was adjusted to 10 in order to avoid the latter effect. In either case, the peak potential, E_p (corresponding to the electroreduction of haloethanols), was found to be independent of the solution pH, consistent with the electron transfer to the carbon−halogen bond being the rate-determining step of the electrode reactions. Gas chromatographic analyses demonstrated ethylene being the main reaction product formed during the iodoethanol and bromoethanol reduction on glassy carbon in near neutral solutions (pH 5.0−7.5). In fact, the bulk electrolysis of 5.45 mM X-EtOH (X = Br, I) at their respective E_p led to the formation of ethylene with only small amounts (5−6%) of ethanol.

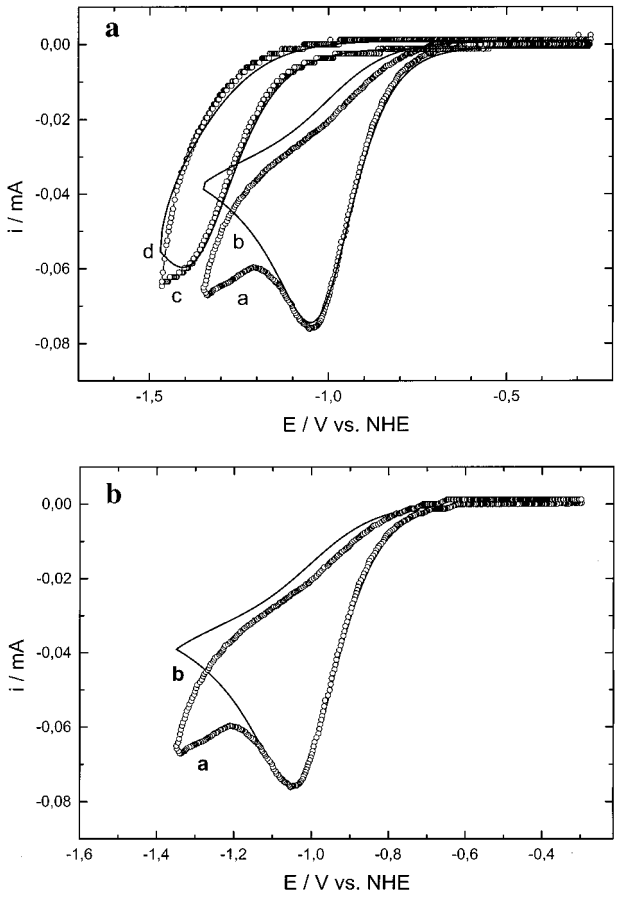

Figure 1. (A) Cyclic voltammograms for the reduction of 5.45 mM solution of 2-iodoethanol (I-EtOH) (a), respectively, 2-bromoethanol (Br-EtOH) (b) recorded at 50 mV s^{-1} on a glassy carbon electrode in aqueous 0.125 M $NaClO_4$/0.01 M phosphate buffer (pH 6.45) electrolyte. (B) Cyclic voltammogram recorded on glassy carbon electrode for 25 mM Br-EtOH in 0.1 M aq. $NaClO_4$ solution (pH 10, adjusted by NaOH). Scan rate: 50 mV s^{-1}. Experimentally obtained voltammograms are shown as circles, their simulations are represented by solid lines.

To understand the dissociative electrochemistry of the above halogen-containing compounds, we have adopted a similar strategy as in the case of methyl and methylene halide

TABLE 1: Electronic Energies and Ideal Gas Thermodynamic Data for Selected Compounds (MP2/6-31G//MP2/6-31G**)**

							theor./exp.[g]		
	symmetry	E_{LUMO} (Hartree)	E_e(MP2/MP4)[c] (Hartree)	ZPE[d] (Hartree)	TCE[e] (Hartree)	S^o (J/K mol)	C_p[f] (J/K mol)	$\Delta_f H^{o(g)}$ (kJ/mol)	$\Delta_f G^{o(g)}$ (kJ/mol)
CH_4	T_d	0.2567	−40.364 626	0.046 449	0.0502599	206.53	34.98	-	-
			−40.385 500			186.30	35.30	−74.4	−50.3
C_2H_4	D_{2h}	0.1782	−78.317 282	0.052 250	0.056 231 7	218.85	41.96	-	-
			−78.344 634			219.60	43.60	52.5	68.4
CH_3Br	C_{3v}	0.166	−2609.811 725	0.038 411	0.0424 106	245.07	41.25	-	-
			−2610.064 600			246.40	42.40	−35.5[h]	−26.3[h]
CH_3I[a]	C_{3v}	0.1004	−6935.759 289	0.037 384	0.0411 453	253.31	42.86	-	-
			−6935.785 995			254.10	44.40	14.7	15.7
Br−CH_2CH_2OH	C_1	0.1578	−2724.026 345	0.073 460	0.0792 684	307.01	74.28	−170.0	−107.8
			−2724.150 650			-	-	−185.3*	−122.7*
I−CH_2CH_2OH[a]	C_1	0.0988	−7049.357 833	0.071 917	0.0779 387	317.73	76.76	-	-
			−7049.397 020			-	-	−150.4 *	−96.4*
CH_3CH_2OH	C_1	0.2252	−154.569 062	0.082 559	0.0877 104	268.17	63.39	-	-
			−154.603 345			273.86	65.40	−235.1	−168.5
·CH_2CH_2OH[b]	C_1	−0.122	−153.884811	0.070 165	0.0744 750	255.00	50.09	−17.1[i]	38.2[j]
						-			
·CH_3[b]	D_{3h}	−0.099	−38.346 013	0.030 042	0.0338 271	186.02	33.81	-	-
			−39.714 750			194.20	38.70	146.9	145.7

[a] Calculated at the MP2/MIDI(d,p) level. [b] Calculated at the ROHF/6-31G** level. [c] Unscaled electronic energy. [d] Unscaled zero-point vibrational energy. [e] TCE = $H°$ (298.15) − $H°$ (0) + ZPE. [f] Constant pressure heat capacity. [g] Experimental values taken from ref 23, except for 2-bromoethanol, respectively, 2-iodoethanol (*) where the enthalpy of formation was calculated from the C−X bond strength reported in ref 15. The molar entropy $S°$ was calculated for the two haloethanols at the MP2/6-31G**, respectively, MP2/MIDI(d,p) level and used subsequently for $\_\Delta_f G^{o(g)}$ calculation. [h] Taken from refs 40−41. [i] Taken from ref 16. [j] Both the geometry of the hydroxyethyl radical (as shown in Figure 2) and the vibrational analysis were done at the ROHF/6-31G** level. Molar entropy $S°$ from the latter calculation, together with known entropies of elements C, H, and O (from ref 23), and $\_\Delta_f H°$ from ref 16, were used to calculate $\_\Delta_f G^{o(g)}$.

reduction.[3,4] First, we have estimated theoretical standard potentials $E^{o(aq)}$ for the chemically irreversible reactions (a−c)

$$Br{-}CH_2{-}CH_2{-}OH(aq) + e^- \rightarrow \cdot CH_2{-}CH_2{-}OH(aq) + Br^-(aq) \quad (a)$$

$$I{-}CH_2{-}CH_2{-}OH(aq) + e^- \rightarrow \cdot CH_2{-}CH_2{-}OH(aq) + I^-(aq) \quad (b)$$

$$\cdot CH_2{-}CH_2{-}OH(aq) + e^- \rightarrow CH_2{=}CH_2(g) + OH^-(aq) \quad (c)$$

and for the minor reaction channel leading to the formation of alcohol

$$\cdot CH_2{-}CH_2{-}OH(aq) + e^- \rightarrow {}^-CH_2{-}CH_2{-}OH(aq) \quad (d)$$

$${}^-CH_2{-}CH_2{-}OH(aq) + H^+(aq) \rightarrow CH_3{-}CH_2{-}OH(aq) \quad (e)$$

Theoretical estimate of the redox potentials was done using a classical approach relying on the dissociation energy[14] of the carbon−halogen bond and, also, directly through ab initio calculations based on isodesmic reactions for the species of interest. Because the apparent hydrophilicity of haloethanols is contrasted by the hydrophobicity of some of the products of their reduction (i.e., ethylene), we used a polarization continuum model (PCM), extended for the calculation of cavitation, dispersion and Pauli repulsion contributions to the solvation free energy,[15] in order to include specific solvation effects in the redox potential calculation.

In the second part of the present work, we address some aspects of the dissociative electron-transfer associated with the electroreduction of haloethanols (i) at polycrystalline copper and silver electrodes, and (ii) at low-index single-crystal Cu(111), Cu(100), Cu(110), and Ag(111) electrodes.

A. Theoretical Estimates of Thermodynamic Parameters. Calculation of redox potentials for the chemically irreversible reactions (a−c) requires a detailed knowledge of gas-phase Gibbs energies of formation for the reactants and reaction products. Furthermore, the Gibbs energy change upon their transfer from the gas phase into the aqueous solution should normally be included in such calculations. Basic procedures leading to an estimate of $E^{o(aq)}$ for methyl and methylene halides have been described in our previous work,[4] and, for comparison, the $\Delta_f G^{o(g)}$ energy values for haloethanols in Table 1 are shown together with those for CH_3Br and CH_3I. Calculated and experimental solvation energies for selected halogen-containing compounds and hydrocarbons related to the present study are summarized in Table 2. The latter includes also related Gibbs energies of formation for all molecules in water, $\Delta_f G^{o(aq)}$, corrected for their hydration energy.

It should be noted that the Gibbs energies of formation ($\Delta_f G°$) for bromoethanol and iodoethanol are not available from the literature. Fortunately, C−Br, respectively, C−I bond dissociation energies (D_o) for these molecules have been reported (280 and 240 kJ/mol, respectively),[16] so that the gas-phase enthalpy of formation ($\Delta_f H^{o(g)}$) can be readily estimated using eq 1 (BDE)

$$D_o = \Delta_f H^o_{(R\cdot)} + \Delta_f H^o_{(X)} - \Delta_f H^o_{(R-X)} \quad (1)$$

Conformational analysis for both haloethanols have been previously done in theoretical works (ab initio) reported by Thomassen et al.[17] and Baumi.[18] Unfortunately, neither of those studies report pertinent thermochemical analysis for the two haloethanols. This prompted us to optimize geometry for 2-bromoethanol using the same level of theory[19] as employed in the latter work, whereas different basis set has been chosen in the case of 2-iodoethanol (vide infra). Most of the molecular geometries (except for iodine-containing compounds) were obtained using the second-order Møller−Plesset (MP2) perturbation theory with the split-valence plus polarization 6-31G** basis set (d-type polarization functions on heavy atoms and p-type on hydrogen). The latter basis set is currently not available for certain heavy atoms, including iodine, so that

TABLE 2: Computed Componenets of Hydration Free Energies of Selected Solutes, ΔG^{o}_{s}

compound/ basis set	del	pol	cav (kcal/mol)	disp	rep	ΔG^{o}_{s} (theor) tot	ΔG^{o}_{s} (exp) (kcal/mol)	$\Delta_f G^{o}$(g) (kJ/mol)	$\Delta_f G^{o}$(aq) (kJ/mol)
CH_4									
MIDI(s,p,d)	0.00	−0.38	6.00	−4.94	1.10	1.78	2.00	−50.3	−41.93
[a]MINI(2s,2p,2d)	0.00	−0.40	6.00	−6.60	2.00	2.00			
C_2H_4									
6-311++G**	0.11	−1.26	7.56	−7.04	2.32	1.59	1.30	68.4	73.84
MIDI(s,p,d)	0.10	−1.23	7.56	−6.59	1.88	1.62			
[a]DZP+s,p,d	0.10	−1.30	7.50	−7.10	1.90	1.90			
CH_3CH_2OH									
[a]DZP(s,p,d)	0.70	−6.80	9.90	−10.00	2.60	−3.50	−5.00	−168.5	−189.42
MIDI++(s,p,d)	0.72	−5.89	10.13	−9.77	2.82	−2.70			
CH_3Br									
MIDI++(s,p,d)	0.62	−3.55	8.43	−7.78	2.38	−0.51	−0.82	−26.3	−29.73
CH_3I									
MIDI++(s,p,d)	0.64	−3.40	9.30	−8.44	2.73	0.19	−0.89	15.66	11.94
$Br-CH_2CH_2OH$									
MIDI++(s,p,d)	0.89	−7.10	12.27	−10.70	3.24	−2.28	-	−122.71	−132.25
$I-CH_2CH_2OH$									
MIDI++(s,p,d)	1.05	−7.54	13.14	−11.32	3.57	−2.16	-	−96.4	−105.43

[a] Taken from ref 15; del = delta internal energy, pol = polarization interaction, cav = Pierotti cavitation energy, disp = dispersion free, tot = total solvation energy, ΔG^{o}_{s}(theor).

related MP2 calculations on 2-iodoethanol and methyl iodide were done using the Huzinaga MIDI basis set (again, extended for d- and p-type polarization functions). For some molecules containing no heavy atoms such as methane, ethylene, and ethanol, we have also optimized molecular geometries employing larger basis sets such as 6-311++G**. The use of diffuse functions has in fact been shown as the most adequate to calculate solvation energies in water, especially, in the case of hydrophobic hydrocarbon molecules.[15]

Electron correlation energy was calculated at the second-, third-, and fourth order Møller−Plesset (MP2-MP4) perturbation theory in the space of single, double, and quadruple excitations (frozen core, MP4−SDQ). This was followed by the calculation of infrared spectra and a complete thermochemical analysis for molecules shown in Table 1 (at 0 and 298.15 K, respectively) to obtain the zero-point vibrational energy (ZPE), the thermal correction, TCE, the constant pressure heat capacity, C_p, and the molecular entropy, $S°$. The enthalpy of formation for 2-bromoethanol, $\Delta_f H^{o(g)}$, was subsequently established at the MP2/6-31G**//MP2/6-31G** level from the isodesmic reaction

$$CH_3Br(g) + CH_3CH_2OH(g) \rightarrow Br-CH_2-CH_2-OH(g) + CH_4(g) \quad (f)$$

The related gas-phase Gibbs energy of formation was then obtained from eq 2

$$\Delta_f G^{o}_{Br-EtOH} = \Delta_f H^{o}_{Br-EtOH} - 298.15[S^{o}_{Br-EtOH} - \Sigma S^{o(elements)}] \quad (2)$$

(where possible, the calculated energies of formation and entropies in Table 1 are compared with the experimentally measured values, in the following column). Because the previous ab initio studies[17,18] have clearly established that the lowest in energy conformers of Br-EtOH and I-EtOH adopt in the gas phase a Gg′ geometry, all our gas-phase calculations for both haloethanols are related to the same Gg′ geometry(cf. Figure 2).

The calculated infrared frequencies for the above-mentioned gas-phase geometries were scaled by apropriate scaling factor of 0.937, whereas ZPE was scaled by 0.9608, as recommended for the MP2/6-31G**.[20] In the case of 2-bromoethanol, a very good agreement was reached between calculated IR frequencies and those reported in ref 17. As can be seen from Table 1, the agreement between the calculated C_p as well as $S°$ and the experimentally measured values is, in general, very good. Somewhat higher calculated values have been found in the case of methane (using the 6-31G** basis set), but the calculated $S°$ value for CH_4 was closer to experiment when using 6−311-G** basis set (∼186 J /K mol). It should be noted that neither $S°$ nor C_p have previously been reported for Br-EtOH or I-EtOH, so that our calculated values cannot be compared with the experimental ones. The estimate of $\Delta_f H°$ for haloethanols, together with reliable $S°$ calculation from the thermochemical analysis, allowed us to obtain $\Delta_f G^{o(g)}$, necessary for the subsequent estimate of the redox potentials for the one-electron reduction of haloethanol to hydroxyethyl radical and halide anion.

According to BDE approach (eq 1), the redox potential for the one-electron reduction of Br-EtOH equals to −0.572 V vs NHE, being somewhat more positive than that for CH_3Br (ca. −0.730 V).[3] Alternative way of estimating $E°$ for bromoethanol is through the above-mentioned isodesmic reaction f, where from the reaction enthalpy $\Delta H(r) = \Delta E_e + \Delta TCE$, and known experimental $\Delta_f H°$ values for EtOH, CH_3Br, and CH_4 (Table 1), one estimates $\Delta_f H^{o}_{(Br-EtOH)} = -170$ kJ/mol. As shown in Table 1, the latter value is somewhat lower than −185 kJ/mol obtained from eq 1. Correspondingly, ab initio calculation leads to a more positive potential for the Br-EtOH reduction, namely, $E° = -0.414$ V. The corresponding $E°$ for the one-electron I-EtOH reduction in water is more negative, namely, −0.782 V.

All the above-mentioned $E°$ values include also hydration energy contribution associated with the X/X^- couple.[21] For haloethanols and hydroxyethyl radical, the gas-phase energies of formation were used. Even though the actual hydration energy for $\cdot CH_2CH_2OH$ radical is not known, one would expect a value similar to that for ethanol (cf. Table 2). In such a case, the net contribution of solvation energies of haloethanol, respectively, $\cdot CH_2CH_2OH$ radical to $E°$ (reactions a−b) would be close to zero.

As already mentioned, the haloethanol reduction on glassy carbon in aqueous solutions apparently does not depend on the solution pH. This situation is analogous to that observed (on the same electrode) during the methyl and methylene halides

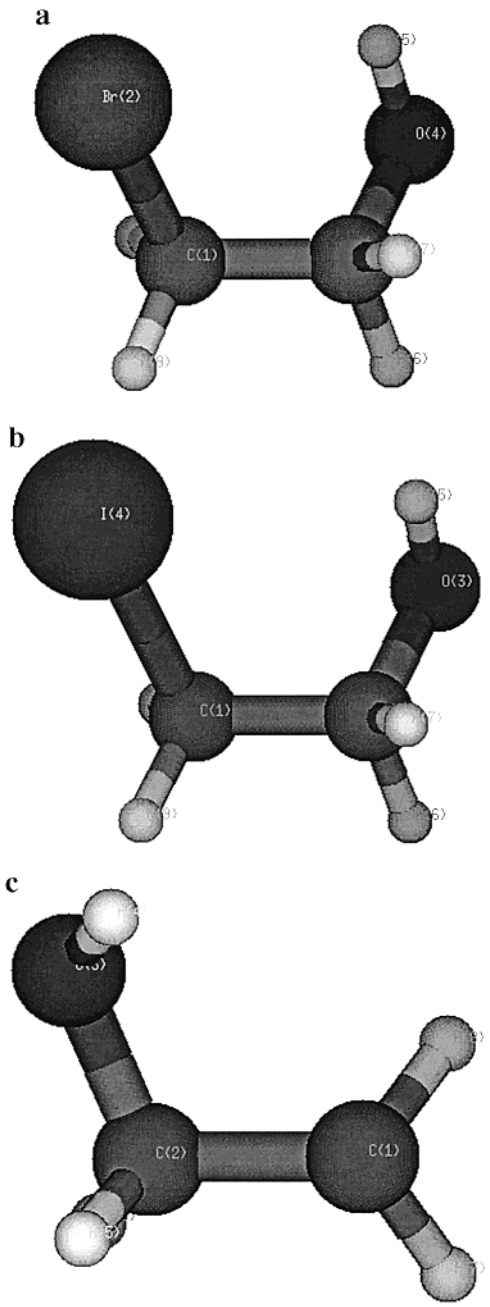

Figure 2. Lowest in energy gas-phase geometries (among several possible rotamers) for 2-bromoethanol (top), 2-iodoethanol (middle) and hydroxyethyl radical (bottom). The dihedral angle XCCO (X = halogen) in the former two molecules was constrained to −63° and the geometries for both molecules have been optimized at the MP2/6-31G**, respectively, MP2/MIDI(p,d) level. The lowest in energy C_1 (^{2}A) geometry for hydroxyethyl radical was obtained at the restricted open shell Hartree−Fock ROHF/6-31G** level and, is similar to that reported in ref 32.

reduction.[3,4] The latter behavior has been assigned to positive electron affinities of methyl radical and carbene (0.08 and 0.65 eV, respectively), both being easier to reduce than the parent molecules. The hydration energies for both of these radicals are unknown, but are expected to be low and similar to that of methane (ca. 2 kcal/mol).

It is interesting to compare energy requirement for the electroreduction in water of 2-hydroxyethyl radical to ethylene and OH^- with that for the $\cdot CH_3$ radical reduction to methane.[3] As shown in Table 1, hydroxyethyl radical possesses LUMO significantly lower than that of methyl radical (as also evident from our restricted open shell ROHF/6-31G** calculations). Because reaction c represents the C−O bond cleavage process, it is more adequate to estimate $E^{o(aq)}$ for the latter reaction in the aqueous solution rather than from the approach relying on the gas-phase energies for C_2H_4 and $\cdot CH_2CH_2OH$ (expected to be quite different because of their differing hydrophilicity). Because the Gibbs energy for reaction c is not known, we have first estimated the bond dissociation energy for the C−O group in $\cdot CH_2CH_2OH$ radical, and subsequently $E^{o(aq)}$, as described in the following text. The corresponding bond dissociation energy D_o(C−O) to give ethylene and ·OH radical, can be obtained from the gas-phase enthalpies of formation at 298.15 K[22]

$$D_o = \Delta_f H^o_{(C_2H_4)} + \Delta_f H^o_{(\cdot OH)} - \Delta_f H^o_{(\cdot CH_2CH_2OH)} \qquad (3)$$

$$52.47 + 39.3 - (-17.1)\ \text{kJ/mol}$$

This leads to an unusually low D_o ∼109 kJ/mol value in comparison with almost 4-fold larger bond strength for the C−O bond in ethanol (395 kJ/mol).[23] As the result, one would expect (considering exclusively thermodynamics and neglecting kinetic effects) quite facile reduction of $\cdot CH_2CH_2OH$ radical to C_2H_4 and OH^- anion. The latter si further facilitated by large, negative hydration energy of OH^- anion (∼ −460 kJ/mol).[21] The redox potential for the reaction c can be determined using eq 4

$$FE^{o\cdot}_{CH_2CH_2OH/\cdot C_2H_4+OH^-} = -D_{o(C-O)} - T(\bar{S}^{\cdot}_{CH_2CH_2OH} - \bar{S}_{C_2H_4} - \bar{S}_{OH\cdot}) + FE^{o}_{(\cdot OH/OH^-)^{aq}} \qquad (4)$$

where $\bar{S}$ represent gas-phase molar entropies for all the species, expressed as a difference $S° - \Sigma S$(elements) at 298.15 K ($S°$ = molar entropy). The latter quantity has not been previously reported for the hydroxyethyl radical. Our estimate of $S°$ (CH_2-CH_2OH) = 255 J/mol K and $\bar{S}^{\cdot}_{CH_2CH_2OH}$ = −183 J/mol K (ROHF/6-31G**), leads to the redox potential for (c) $E°$ = +1.545 V vs NHE. The latter $E°$ does not include specific hydration energies for the hydroxyethyl radical and ethylene, respectively. A more exact estimate of the redox potential for reaction c should be based on the equation

$$FE^{o\cdot}_{CH_2CH_2OH/\cdot C_2H_4+OH^-,aq} = \Delta_f G^{o,aq\cdot}_{CH_2CH_2OH} - \Delta_f G^{o,aq}_{C_2H_4} - \Delta_f G^{o,aq}_{OH^-} \qquad (5)$$

Because the Gibbs energy of hydration for the $\cdot CH_2CH_2OH$ radical is unknown, one could assume a similar value as for ethanol (−21 kJ/mol). As shown in Table 2, the hydration energy of ethylene is positive and quite low (5.4 kJ/mol). Consequently, the $E°$ estimate based on eq 5 is ca. −0.16 V more negative than that neglecting the hydration energies of ethylene and $\cdot CH_2CH_2OH$ radical. These results suggest that the reductive cleavage of hydroxyethyl radical in aqueous solution is thermodynamically very facile. The main reason is a very low D_o for the C−O bond. This, in turn, is expected to favor its fragmentation, upon reduction, to ethylene and OH^- rather than the reaction sequence (d−e) leading to ethanol formation.

For the purpose of comparison, we have also included in Table 2 theoretical estimates of $\Delta G°_s$ for CH_4, C_2H_4 and CH_3-CH_2OH reported by Amovilli and Mennucci.[15] Even though the present work reproduced general trends of the latter work and individual contributions of repulsion, cavitation and polarization

terms into the total solvation energy, more or less important differences in ΔG^{o}_{s}(theor) are likely to result from different choice of basis sets in both studies. It should also be noted that the hydration energy estimate for ethanol is lower than the experimental value in both instances. One may also note that we have failed to reproduce negative (even though small) solvation energy for methyl iodide (as found experimentally). Therefore, we consider the hydration energy estimates for both haloethanols in the present study as preliminary, even though one may expect somewhat lower hydration energies for Br-EtOH and I-EtOH than for ethanol (as found in our calculation). Currently, we are attempting to perform similar solvation studies for halocarbons and haloethanols by means of Miertus−Scrocco−Tomasi model and Pierotti−Claverie method[15] using MIDI! basis set, recently optimized for both bromine as well as iodine atoms[24] The latter basis set, when combined with ab initio methods, gave an excellent agreement between the theory and experiment for a number of organic halide molecules.[25−29]

B. Kinetics of Haloethanol Reduction on Glassy Carbon Electrodes. As evident from Figure 1, the electroreduction of both haloethanol molecules is feasible on glassy carbon, iodoethanol being easier to reduce than bromoethanol by ca. 0.36 V. The corresponding reduction peak E_p potentials are ca. 0.270 V, respectively, 0.84 V more negative than the BDE-based $E°$ estimates. Relatively large shift of the reduction potential of bromoethanol with respect to the theoretical $E^{o(aq)}$ is, apparently, due to a quite sluggish heterogeneous ET kinetics of the latter process. This is partially due to a significant reorganization energy coming from both, the bond dissociation energy of ca. 2.9 eV, as well as the solvent reorganization energy (ca. 1.0−1.6 eV).[3] According to the Savéant DET model, the overall barrier for the ET process at the transition state should be simply one-fourth of their respective sum, ca. 0.9−1.1 eV. This is expected to result in reaction overpotentials approaching 2 V, much larger than those observed in the present work. In fact, our simulations of cyclic voltammograms[30] (Figure 1, solid line) gave the apparent rate constant for the one-electron reduction of 2-bromoethanol $k^{o'} = 5.8 \times 10^{-7}$ cm/s ($\alpha = 0.28$), the 2-iodoethanol reduction being much faster ($k^{o'} = 1 \times 10^{-4}$ cm/s, $\alpha = 0.36$). Note that practically the same data concerning ET kinetics associated with 2-bromoethanol were extracted from the experimental data shown in Figures 1A and B for the reduction of both 5.45 mM and 25 mM BrEtOH solutions. According to the predictions of DET model,[5] the electroreduction of 2-bromoethanol, or that of methyl bromide ($D_o = \sim 280$ and 290 kJ/mol, respectively) should occur far in the hydrogen evolution region, at potentials as negative as −2 V. The fact that the actual kinetics are much faster may be tentatively assigned to the solvent effect on the transition state (TS) formed during the ET-induced cleavage of haloethanol molecules. This issue is not treated explicitely in the present work because the ab initio methods are less suitable for modeling the dissociative bond breaking processes. On the other hand, multiconfigurational self consistent field (MCSCF) method would be more appropriate to study the solvent effect on TS, however, the latter becomes prohibitively expensive and time consuming considering the number of electrons contained in both haloethanol molecules. Effects of water on the TS formed during the reductive cleavage of $\cdot CH_2CH_2OH$ radical to ethylene and hydroxyl anion and related ET kinetics will be addressed in our future quantum chemical studies.[31]

Although the hydroxyethyl radical reduction is not perceptible directly from the electrochemical data, its involvement is confirmed indirectly through the GC analysis of the reaction products (ethylene formation) coming from haloethanol reduction. The geometry of the hydroxyethyl radical in the gas phase[22,32] as well as that of the corresponding transition state formed during its cleavage into ethylene and ·OH radical have been studied at the UHF/6-31G* level by Sosa and Schlegel.[33,34] In contrast to the equilibrium state of the $\cdot CH_2CH_2OH$ radical (cf. Figure 2), its TS appears as a planar structure, necessary for the rehybridization of the methylene carbons from sp3 to sp2. In the gas phase, the formation of the transition state is accompanied by the increase in the C−O bond length by ca. 0.8 Å and a decrease of the OCC angle from 113° to 105°. As the radical reorients toward its TS geometry, the moment of inertia increases, and the rotational energy is expected to be transferred into the nuclear motions (vibrations) of the radical.[16] A similar type of sp3-sp2 rehybridization and TS formation will be also required to occur in aqueous solution, and one would expect significant degree of TS stabilization by water molecules (dipole−dipole interactions and hydrogen bonding) and, especially, due to large stabilization of the leaving group (hydroxyl anion) by water molecules. The one-electron reduction of hydroxyethyl radical in aqueous solution is expected to involve non negligible contribution of nuclear reorganization energy into the overall energy barrier for the electron transfer process. This should include not only the inner-shell reorganization energy coming from the C−O bond cleavage (109 kJ/mol) but, also, the rehybridization of methylene carbons accompanied by carbon−carbon bond shortening (in order to form ethylene). Due to high polarizability of water ($\epsilon = 78$), a significant outer-shell reorganization energy is also expected (more than 1 eV). This, in turn, is expected to lead to a relatively large shift of the E_p potential for the one-electron $\cdot CH_2CH_2OH$ reduction to ethylene and OH^- anion with respect to $E°$ for the reaction 5.

C. Dissociative Haloethanol Reduction on Low-Index Single-Crystal Ag and Cu Electrodes. It has already been mentioned that small amounts of ethanol were produced during haloethanol electrolysis on glassy carbon electrode in neutral solutions. The ethylene and ethanol formation on glassy carbon can be assumed to involve outer-shell ET steps, presumably without any assistance of the electrode surface. However, one would expect the reaction mechanism and kinetics to change when replacing the carbon by group IB metal cathodes, as noticed previously in the case of methyl and methylene halide reductions.[3,4] As already mentioned in the Introduction section, thermal activation of both 2-bromoethanol and 2-iodoethanol on Ag(111) and Ag(110) in the gas phase has been reported to produce, among other reaction products, significant amounts of acetaldehyde.[9,10] However, no surface-assisted coupling of hydroxyethyl radicals to 1,4-butanediol was noted. This prompted us to check whether in purely aqueous solution one could achieve efficient coupling of $\cdot CH_2CH_2OH$ radicals without using any solution phase catalyst (cf. refs 6−7). For this purpose, a series of bulk electrolyses of haloethanol solutions on Ag and Au electrodes were coupled to GC analyses. Two types of GC/FID experiments were performed; those at 150 °C allowed us to follow quantitatively volatile gaseous products at the outlet of the electrochemical cell, whereas those at 250 °C, involving injection of electrolyzed solution, gave concentrations of water-soluble products such as ethanol and iodoethanol (little present in the gas phase due to their high solubilities in water). Figure 3A shows practically linear GC responses for ethanol, respectively, 2-iodoethanol standard solutions prepared in the supporting electrolyte used for the electrolyses of haloethanol (the slope being ca. 2-fold larger for ethanol compared to I-EtOH). In Figure 3B are displayed gas chromatograms recorded for the

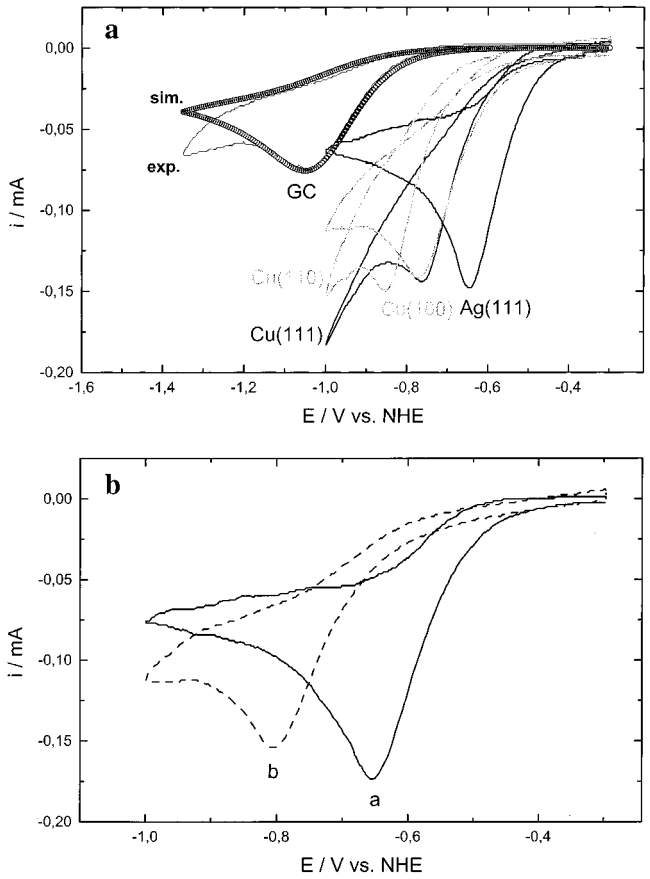

Figure 3. (A) Gas chromatographic (GC/FID, Haysep R column) response to injections (1 μL) of various amounts of ethanol (a) and I-EtOH (b) dissolved in 0.125 M $NaClO_4$/0.01 M phosphate buffer (pH 6.45) aq. electrolyte. **(B)** Gas chromatographic traces for the electrolyte solution containing 50 mM I-EtOH before electrolysis (a), and following electrolysis of the haloethanol on polycrystalline Cu at −0.70 V for 200 min (b). During the injections, both detector and injector were kept at 250 °C.

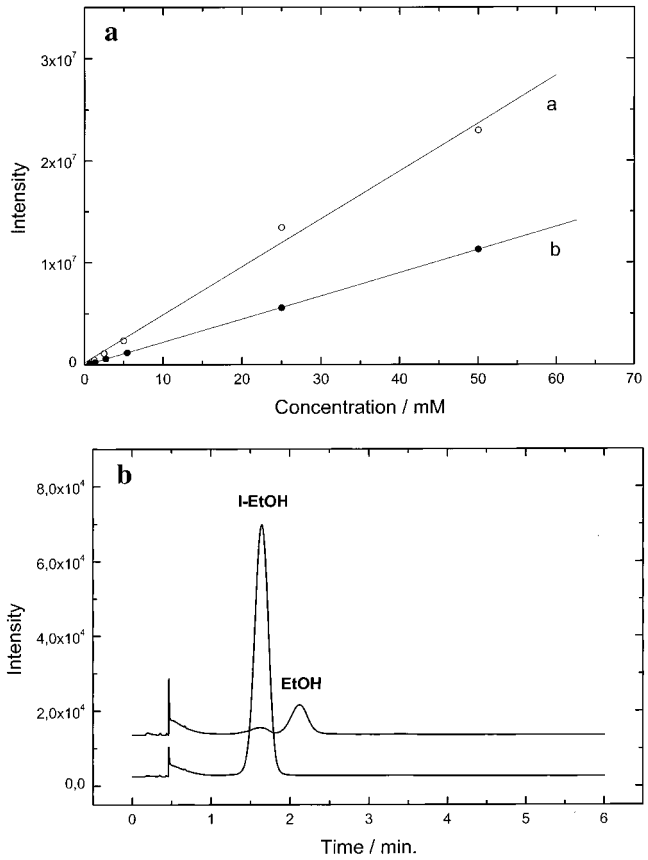

Figure 4. Gaseous products formed during constant-potential electrolyses of the 5.45 mM solution of I-EtOH on polycrystalline Cu as a function of the electrode potential: −0.70 (a), −0.81 (b), −0.91 (c), and −1.10 V (d). The cathodic compartment of the cell was purged with argon at a rate of 8.5 mL/min and analyzed using a FID detector at 150 °C. Electrolysis time: at least 15 min at each electrode potential were allowed before each GC injection of the sample.

starting 50 mM I-EtOH solution (curve a) and following its electrolysis on a large area Cu cathode at −0.8 V for 200 min (curve b). Inspection of the GC data showed an almost complete destruction of iodoethanol (97%), with only 4.4% of the consumed I-EtOH molecules being converted into ethanol. At the same time, GC/FID measurements conducted at 150 °C revealed large amounts of ethylene formed during electrolyses with practically no trace of methane, or ethane. In addition, in some electrolysis runs, small amounts of highly volatile acetaldehyde were detected. However, at any electrode potential studied, CH_3CHO yields barely exceeded 1% of the total amount of the reaction products. Formation of ethanol during electroreduction of 25 mM I-EtOH was also confirmed through Raman measurements in solution (data not shown).[38] The latter measurements showed also that the electrolyses conducted at a Cu electrode did not lead to detectable amounts of 1,4-butanediol. This claim is further supported by detailed analysis of the GC data (Figure 4) recorded for the gaseous products formed during electrolyses of 5.45 mM I-EtOH as a function of the electrode potential. In the latter case, the cell was continuously purged with argon at the rate of 8.45 mL/min. The amount of ethylene first increased reaching a maximum at ca. −0.9 V, and then dropped down at potentials negative to −1 V due to the onset of hydrogen evolution. The maximum faradaic yield for ethylene production exceeded 90%. The ethanol yields on copper were in general larger at more positive potentials (close to the onset potential for iodoethanol reduction), but did not exceed 10%. The latter figure is comparable to that found following similar electrolyses conducted on glassy carbon at −1.0 V, where 5.45 mM of 2-iodoethanol were converted to ethylene and 0.24 mM of ethanol.

Figure 5A shows cyclic voltammograms for the electroreduction of 2-iodoethanol on low-index single-crystal Cu and Ag electrodes, whereas voltammograms recorded on polycrystalline metals are shown in Figure 5B. The C−I bond activation in iodoethanol appears the most facile energetically on Ag(111) and on polycrystalline silver. Under such conditions, the iodoethanol reduction occurs at a potential ca. 0.4 V more positive than on glassy carbon. The E_p potential is ca. 120−130 mV more negative on Cu(111) and on Cu(100) than on a Ag(111) electrode, and undergoes further negative shift on a Cu(110) electrode. Iodoethanol reduction on polycrystalline copper (Figure 5B, curve b) occurs in a similar potential range as on Cu(110). The surface of the latter can be characterized by so-called missing-raw structure, whereas the polycrystalline material is thought to consist of patches of a number of crystallographic planes, certain of them being more preferred than the others. Even though there exists a clear E_p shift for haloethanol reduction at different crystal faces of copper, the question arises to what extent the observed behavior is related to differing kinetics of haloethanol cleavage (i.e., related to the molecular structure of 2-iodoethanol and/or radicals formed upon its reduction), and to what extent the latter is due to the "substrate" effects (i.e., adsorption of electrogenerated halide

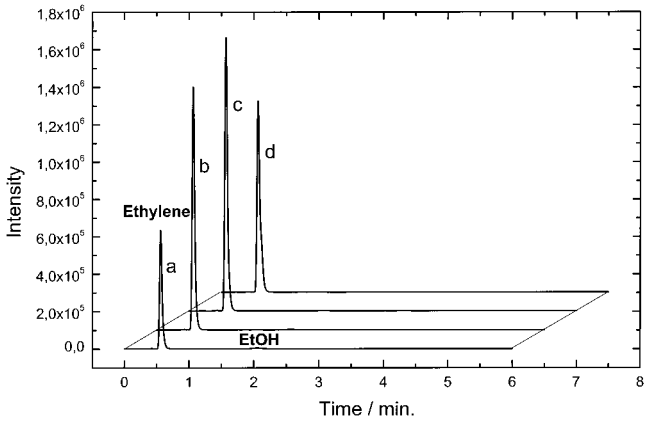

Figure 5. (A) Cyclic voltammograms for the reduction of 5.45 mM aq. I-EtOH recorded on low-index Cu single-crystal and Ag(111) electrodes compared with the experimental CV recorded on glassy carbon (exp) and its simulation using Antigona software (sim.). Scan rate: 50 mV s^{-1}. All other experimental conditions as in Figure 1A. (B) CV curves recorded for 5.45 mM aq. I-EtOH on polycrystalline Ag (a) and Cu (b) electrodes. Other conditions as in Figure 1A.

anions on metal surface affecting thus electronic structure of the metal as well as the charge distribution at the electrode/solution interface). It became clear from our previous study[3] that both phenomena are interlinked and cannot be easily separated (unless the reduction process would occur at highly negatively charged electrodes where halide anion adsorption would be limited, or completely prevented). Importantly, halogen adsorption cannot be eliminated when studying thermally induced activation of haloethanols or halogenated hydrocabons in the gas phase. Under UHV conditions, the Fermi level in metal is tuned by varying surface coverage of carbon-containing radicals as well as halides generated during the cleavage of carbon−halogen bond. It is evident that the latter will affect both the extent of metal-to-adsorbate charge transfer (or opposite) as well as the mobility of radicals on the metal surface.[12] For example, photodissociation of methyl halide (occurring at ca. 200−420 nm) on a Ag(111) surface results in adsorbed $\cdot CH_3$ radicals which recombine below 300 K to form ethane. Interestingly, chemisorbed halogen atom is retained on the silver surface to temperatures above 700 K, where it gets ejected into the gas phase as silver halide, rather than halogen.[35] The situation is somewhat different at silver (or copper)/solution interface because electrogenerated halide anions will undergo very fast desorption/readsorption equilibria, as recently demonstrated in the case of Ag(111) electrode[36] for the potential range where haloethanol undergoes electroreduction.

There exist several indications suggesting that the metal surface is involved in the electroreduction of 2-iodoethanol. First, the reduction peak for this molecule is about 0.4 V more positive on silver than on glassy carbon electrode. Second, the E_p potential recorded for the one-electron reduction of 5.45 mM I-EtOH on Ag(111) is ca. 0.1 V more positive than the theoretical $E°$ estimate (note that even assuming some margin of error in our $E°$ estimate, relatively large inner-shell reorganization energy for the latter molecule should cause E_p displacement by hundreds of mV from $E°$, opposite to that actually observed). Furthermore, the cathodic peak current on copper and silver electrodes is ca. 50% larger than on glassy carbon. Simulations of cyclic voltammograms recorded during the I-EtOH reduction on Ag(111) have shown that the magnitude of the peak current can be reproduced providing one would select the diffusion coefficient for I-EtOH on the order of 1.1×10^{-5} cm^2/s, i.e., slightly lower than for ethanol, 1.24×10^{-5} cm^2/s [23] (the decrease in D_{ox} by 11% is quite reasonable considering the size of bulky iodine atom in I-EtOH). On the other hand, it would be difficult to explain 50% decrease in the diffusion limiting current on glassy carbon compared to metal electrodes exclusively due to hydrogen−iodine substitution in ethanol (cf. Figure 5A).

The probability (P_o) with which the activated complex is formed, and electron crosses the energy barrier, can be given[37] as

$$P_o = 1 - \exp[(-|H_{RP}|^2/(h\nu_n)(\pi^3/\Delta G^* RT)^{1/2}] \qquad (6)$$

where the electronic coupling matrix element $|H_{RP}|^2$ expresses the effective electronic-coupling strength betwen the reactant and product in the transition state, h is the Planck constant, ν_n is the nuclear frequency at which the activated complex is formed and ΔG^* is the sum of the inner-shell and outer-shell Gibbs reorganization energies. Providing the activation of haloethanol molecules (i.e., C−X bond cleavage) would occur at a very small distance from the electrode surface (within several angstroms), the electronic transmission coefficient (κ)

$$\kappa = 2P_o/(1 + P_o) \qquad (7)$$

would be equal unity, and the ET kinetics would be highly adiabatic. The standard heterogeneous rate constant (k_o) is then proportional to the magnitude of the total Gibbs reorganization energy, ΔG^*

$$k_o = \kappa K_p \exp(-\Delta G^*/RT) \qquad (8)$$

where $\kappa = 1$ and K_p represents the term determined by the work to be done on the system in order to bring reactant molecules to the reaction plane, rp (also, to remove product molecules from rp). Now, lets consider the case where reduction of I-EtOH takes place at a negatively charged glassy carbon electrode, i.e., at electrode potentials exceeding −1.0 V. Because glassy carbon becomes negatively charged at ∼+0.02 V vs NHE, the transition state associated with the C−I bond cleavage cannot be formed at a short distance from the electrode surface because both halide and hydroxide anions (negatively charged reaction products) will be then strongly electrostatically repelled. As a result, the activated complex will be formed with much lower probability due to the decrease in the maximum electronic overlap, $|H_{DA}\text{-eff}|^2$, between the wave functions of propagating electrons at the Fermi level (donor states in the electrode) and the acceptor states in haloethanol molecule. Such nonadiabacity of electrode reactions is expected to lead not only to a decrease in the heterogeneous rate constant, k_o, but also to a sensible decrease in the cathodic peak current. Note that in order to obtain the agreement between the simulated and experimental cyclic voltammogram for the reduction of 5.45 mM I-EtOH on glassy carbon (Figures 1A, respectively, 5A), the diffusion coefficient as low as 5×10^{-6} cm^2/s had to be used. This is ca. 50% lower than expected theoretically. Thus, the main driving force for extremely fast kinetics of haloethanol reduction on metal electrodes seems to be the stabilization of I^-, respectively, OH^- anions by adsorption at the positively charged silver, respectively copper electrodes, which does not occur on the negatively charged glassy carbon.

IV. Conclusions

Despite the similarity of haloethanol reduction products on glassy carbon and at the metal electrodes, there are large differences in the kinetics of these reactions associated with

the extent of stabilization of the intermediates (and products) resulting from the ET-induced haloethanol cleavage. Apparently, the obtained kinetic data on haloethanol reduction on metal as well as carbon electrodes cannot be interpreted within the framework of the classical DET model.[5] More sophisticated approaches relying on quantum chemical treatment of the problem, accounting correctly for metal−adsorbate interactions as a function of the electrode potential are clearly required.

Acknowledgment. We are indebted to M. Odziemkowski for the measurements of solution Raman spectra. Helpful discussions with J. Mareda are gratefully acknowledged. This work was supported by the Swiss National Science Foundation.

References and Notes

(1) Hori, Y.; Murata, A.; Takahashi, R. *J. Chem. Soc. Faraday Trans. I* **1989**, *85*, 2309.
(2) Fedurco, M.; Jorand Sartoretti, C.; Augustynski J. *J. Am. Chem. Soc*. **1999**, *121*, 888.
(3) Fedurco, M.; Jorand Sartoretti, C.; Augustynski, J. *Langmuir* **2001**, *17*, 2380.
(4) Fedurco, M.; Jorand Sartoretti, C.; Augustynski, J. *J. Phys. Chem. B* **2001**, *105*, 2003.
(5) Savéant, J.-M. *J. Am. Chem. Soc.* **1987**, *109*, 6788.
(6) Cipris, D. *J. Appl. Electrochem.* **1978**, *8*, 545.
(7) Butler, A. L.; Peters, D. G. *J. Electrochem. Soc.* **1997**, *144*, 4212.
(8) Cumbo, C. C. Alkanediols by electrochemical coupling of halohydrins 1982. U. S. Patent No. US 4324625.
(9) Scott, J. G.; Barteau, M. A. *J. Vac. Sci. Technol. A* **1997**, *15*, 1667.
(10) Wu, G.; Stacchiola, D. S.; Kaltchev, M.; Tysoe, W. T. *Surf. Sci.* **2000**, *463*, 81.
(11) Lin, J.-L.; Chiang, C.-M.; Jenks, C. J.; Yang, M. X.; Wentzlaff, T. H.; Bent, B. E. *J. Catal.* **1994**, *147*, 250.
(12) Bent, B. E. *Chem. Rev.* **1996**, *96*, 1361.
(13) Smolinski, S.; Sobkowski, J. *J. Electroanal. Chem.* **1999**, *463*, 1.
(14) Savéant, J.-M. *Acc. Chem. Res.* **1993**, *26*, 455.
(15) Amovilli, C.; Mennucci, B. *J. Phys. Chem. B* **1997**, *101*, 1051.
(16) Sapers, S. P.; Hess, W. P. *J. Chem. Phys.* **1992**, *97*, 3126.
(17) Thomassen, H.; Samdal, S.; Hedberg, K. *J. Phys. Chem.* **1993**, *97*, 4004.
(18) Buemi, G. *J. Chem. Soc. Faraday Trans.* **1994**, *90*, 1211.
(19) General description of GAMESS can be found in: Schmidt, M. W., Baldridge, K. K.; Boatz, J. A.; Elbert, S. T.; Gordon, M. S.; Jensen, J. H.; Koseki, S.; Matsunaga, N., Nguyen, K. A.; Su, S. J.; Windus, T. L.; Dupuis, M.; Montgomery, J. A. *J. Comput. Chem*. **1993**, *14*, 1347. All the ab initio calculations and solvation modelling studies were performed on a 667 MHz PC (Pentium III, 128 Mb RAM) using Gamess(US) (Version 6.0, compiled 01−07−2000 by Alex. A. Granovsky).
(20) Scott, A. P.; Radom, L. *J. Phys. Chem.* **1996**, *100*, 16 502.
(21) Savéant, J.-M. *J. Phys. Chem.* **1994**, *98*, 3716.
(22) Espinosa-García, J. *Chem. Phys. Lett.* **1997**, *278*, 209.
(23) *CRC Handbook of Chemistry and Physics*; 76th ed., Lide, D. R.; Frederikse, H. P. R., Eds., CRC Press: Boca Raton, FL, 1995.
(24) Easton, R. E.; Giesen, D. J.; Welch, A.; Cramer, C. J.; Truhlar, D. G. *Theor. Chim. Acta*, in press (available at EMSL Basis Set Library).
(25) Li, J.; Hawkins, G. D.; Cramer, C. J.; Truhlar, D. G. *Chem. Phys. Lett.* **1998**, *288*, 293.
(26) Zhu, T.; Li, J.; Hawkins, G. D.; Cramer, C. J.; Truhlar, D. G. *J. Chem. Phys.* **1998**, *109*, 9117.
(27) Hawkins, G. D.; Cramer, C. J.; Truhlar, D. G. *J. Phys. Chem. B* **1998**, *102*, 3257.
(28) Cramer, C. J.; Truhlar, D. G. *Chem. Rev.* **1999**, *99*, 2161.
(29) Li, J.; Zhu, T.; Cramer, C. J.; Truhlar, D. G. *J. Phys. Chem. A* **2000**, *104*, 2178.
(30) Antigona CV simulation software package was kindly provided to us by Dr. L. Mottier (University of Bologna, Italy).
(31) Fedurco, M.; Augustynski, J., manuscript in preparation.
(32) Curtiss, L. A.; Lucas, D. J.; Popple, J. A. *J. Chem. Phys.* **1995**, *102*, 3292.
(33) Sosa, C.; Schlegel, H. B. *J. Am. Chem. Soc.* **1987**, *109*, 4193.
(34) Sosa, C.; Schlegel, H. B. *J. Am. Chem. Soc.* **1987**, *109*, 7007.
(35) Zhou, X.-L-; White, J. M. *Surf. Sci.* **1991**, *241*, 259.
(36) Stevenson, K. J.; Gao, X.; Hatchett, D. W.; White, H. S. *J. Electroanal. Chem.* **1998**, *447*, 43.
(37) Newton, M. D.; Sutin, N. *Ann. Rev. Phys. Chem.* **1984**, *35*, 437.
(38) Solution Raman spectra for 25 mM 2-iodoethanol and one of the reaction products, namely, ethanol, formed during the bulk electrolysis of haloethanol on a polycrystalline Cu electrode (−0.90 V, 200 min) were obtained using a confocal Labram I microscope (air cooled CCD detector, 20 mW HeNe 628.2 nm laser) in the backscattering geometry.
(39) East, A. L. L.; Radom, L. *J. Chem. Phys.* **1997**, *106*, 6655.
(40) Paddison, S. J.; Tschuikow-Roux, E. *J. Phys. Chem. A* **1998**, *102*, 6191.
(41) Paddison, S. J., Tschuikow-Roux, E. *Int. J. Thermophysics* **1998**, *19*, 719.